

# Self-interference Modeling and Digital Cancellation Along with Full-Duplex Wireless System Analysis

(Invited Paper)

Dani Korpi, Taneli Riihonen, Lauri Anttila, and Mikko Valkama

Laboratory of Electronics and Communications Engineering, Tampere University of Technology, Finland  
{dani.korpi, taneli.riihonen, lauri.anttila, mikko.e.valkama}@tut.fi

**Abstract**—This paper highlights recent contributions on the inband full-duplex (IBFD) technology by providing an overview of the related research carried out at Tampere University of Technology, Finland, thus far. In particular, we consider the challenges caused by the own transmitter, which is now a powerful source of self-interference, while also discussing a potential system-level application of the IBFD technology. The former issue is analyzed by presenting advanced signal models for canceling the SI in the digital domain of the receiver. The signal models are derived such that they take into account the most significant analog impairments. As for the system-level application, we propose a self-backhauling IBFD-capable access node that can serve users and backhaul data using the same frequency resources at the same time. This reduces transmit power consumption over the reference scheme that relies on half-duplex operation. Altogether, the findings reported here and in the first author’s dissertation demonstrate that the IBFD technology can significantly enhance the spectrum usage of the future wireless networks.

## I. INTRODUCTION

Inband full-duplex (IBFD) communications, where a radio device transmits and receives simultaneously on the same spectrum, is a recent paradigm shift in wireless communications [1]. Compared to all existing systems, where transmission and reception is divided either in time or frequency, IBFD can even double spectral efficiency, making it a potential solution for obtaining the data rate requirements of the future wireless systems. However, in order to make the concept feasible, the self-interference (SI) problem must first be solved. Namely, in an IBFD radio, the receiver (RX) chain will suffer from powerful interference that is caused by its own transmitter (TX) chain simultaneously operating on the same frequency band. Due to the close proximity of the TX and RX chains, the power of the SI is extremely high, meaning that it must be suppressed by as much as 100 dB to facilitate the reception of actual information signals. To this end, various promising SI cancellation solutions have been recently proposed [2]–[7].

This invited paper provides a brief overview of the doctoral dissertation in [3] and the related works in [4]–[10]. As for the architecture required for SI suppression, the main focus is on digital cancellation. In particular, we discuss alternative signal models required for modeling and reconstructing the SI in the digital domain when operating under analog impairments distorting the SI signal. In addition, example measurement results of two prototype implementations and theoretical system-level performance results are also provided to evaluate the proposed concepts under real-life circumstances.

## II. THE SELF-INTERFERENCE CHALLENGE AND DEVELOPMENT OF ACCURATE SIGNAL MODELS

The main challenge to tackle in making IBFD radio transceivers a reality is to suppress the powerful SI, as mentioned above. Even though there is always some inherent physical isolation between the TX and RX chains, provided by the path loss between separate antennas, or by a circulator if using a single antenna, further active cancellation is needed to fully eliminate the effect of the SI. The predominant technique is to perform the active cancellation in two stages: first before the RX chain using radio frequency (RF) electronics, and then after the RX chain using digital signal processing.

The main purpose of the RF canceller is to make sure that the SI signal is within the dynamic range of the RX chain. This is usually realized by a multi-tap RF canceller that aims at reproducing and canceling the direct leakage between the TX and RX chains. The prevalent option is to use the TX output signal for regenerating the SI signal at this stage, although it is also possible to generate the RF cancellation signal digitally by using an auxiliary TX chain. However, the drawback of the latter option is that it cannot suppress the TX-induced impairments as they are not included in the cancellation signal, unlike when using the actual TX output signal for reconstructing the SI.

Having successfully performed the RF cancellation, the RX chain is not saturated and the overall signal can be digitized with sufficient accuracy. After this, digital SI cancellation is performed. It involves first estimating the necessary coefficients of the used signal model, after which the observed SI is reconstructed and cancelled. In order to fully suppress the remaining SI, the signal model must be sufficiently accurate, that is, it must capture all the distortions that the TX signal experiences in the transceiver. This includes the wireless multipath propagation channel, but also all the analog impairments inherently present in the transceiver chain.

As shown in [3], the most significant impairments are the power amplifier (PA)-induced nonlinear distortion and possibly also the I/Q imbalance. Therefore, in this paper, we present three alternative signal models for the SI: a linear signal model, a widely linear signal model, and a nonlinear signal model. The first is the reference case that does not model any of the impairments, the second captures the I/Q imbalance, and the last models the nonlinearity of the PA. Their unknown parameters are estimated in the next section.

We start from *the linear signal model* that is expressed as

$$y_{\text{LIN}}(n) = \sum_{m=-M_1}^{M_2} h_m x(n-m), \quad (1)$$

where  $x(n)$  is the baseband transmit signal,  $h_m$  denotes the unknown coefficients of the signal model,  $M_1$  is the number of pre-cursor memory taps, and  $M_2$  is the number of post-cursor taps. Pre-cursor memory is introduced in order to accurately model also the fractional delays occurring within the system, alongside with other unforeseen memory effects.

The linear model captures the wireless coupling channel and any other frequency selectivity within the transceiver chain but it is not capable of reconstructing a SI signal that is distorted in any other way. As opposed to this, the widely linear model can also accurately reconstruct SI when the transceiver suffers from I/Q imbalance. This is a common problem in many low-cost transceivers that cannot be properly calibrated [3], [4].

*The widely linear signal model* is defined as

$$y_{\text{WL}}(n) = \sum_{m=-M_1}^{M_2} [h_{1,m}x(n-m) + h_{2,m}x^*(n-m)], \quad (2)$$

where the unknown coefficients are now represented by  $h_{1,m}$  and  $h_{2,m}$  while  $(\cdot)^*$  denotes the complex conjugate. As explained in [3], [4], I/Q imbalance results in the complex conjugate of the original signal being superposed on top of it, and therefore the widely linear model in (2) is capable of regenerating the SI also in such a scenario.

However, often the most significant source of impairment is in fact the transmitter's PA, which is distorting the TX signal heavily in a nonlinear manner. Neither the linear nor the widely linear signal model can accurately reconstruct a nonlinearly distorted SI signal, for which reason the nonlinear signal model is in many cases the preferable option.

Using a parallel Hammerstein (PH) model for the nonlinear PA, *the nonlinear signal model* can be written as follows:

$$y_{\text{NL}}(n) = \sum_{\substack{p=1 \\ p \text{ odd}}}^P \sum_{m=-M_1}^{M_2} h_{p,m} |x(n-m)|^{p-1} x(n-m), \quad (3)$$

where  $P$  is the nonlinearity order and  $h_{p,m}$  represents the unknown coefficients of the  $p$ th-order term. While this signal model does not consider the I/Q imbalance, it is very accurate in canceling SI in devices with low-cost PAs [5], [6], [11].

In the following, we discuss how to perform the estimation of the unknown coefficients present in the above signal models.

### III. PARAMETER ESTIMATION AND ADAPTIVE DIGITAL CANCELLATION

A widely used solution for estimating the unknown coefficients of a signal model is to employ the least mean squares (LMS) parameter learning algorithm, which has been described and evaluated in [3], [5], [6], [12]. To facilitate a uniform notation for each considered signal model, let us first define the so-called *instantaneous basis function vector*. For the linear signal model, it is simply the original transmit signal,

i.e.,  $\psi(n) = x(n)$ . Correspondingly, the instantaneous basis function vector of the widely linear signal model contains also the complex conjugate of the transmit signal, and it is therefore defined as  $\psi(n) = [x(n) \ x^*(n)]$ . Finally, for the nonlinear signal model, the instantaneous basis function vector is

$$\psi(n) = [x(n) \ |x(n)|^2 x(n) \ \cdots \ |x(n)|^{P-1} x(n)].$$

That is, it contains all the nonlinear terms as defined by (3).

Considering then the coefficient estimation problem, before the actual parameter learning, the different basis functions must be orthogonalized. The reason for this is the poor convergence performance of the LMS algorithm if the elements of the input vector are highly correlated, caused by the large eigenvalue spread of the input signal covariance matrix [12], [13], [14, p. 417]. This is especially crucial for the nonlinear signal model, since in that case the static basis functions can indeed be expected to be correlated as they are all dependent on the original transmit signal. The orthogonalization can be done with a matrix that can be obtained as described in [3], [6], [12]. Denoting the orthogonalization matrix by  $\mathbf{S}$ , the static basis functions can then be orthogonalized simply by

$$\tilde{\psi}(n) = \psi(n)\mathbf{S}. \quad (4)$$

Note that the orthogonalization matrix  $\mathbf{S}$  only depends on the statistical properties of the original transmit signal (via the covariance matrix) and hence it does not change with respect to time, as long as the transmit waveform remains the same [3]. This means that the orthogonalization matrix can be precomputed offline, and only the actual orthogonalization in (4) must be performed in real time. However, it is also possible to calculate the orthogonalization matrix adaptively during the actual digital cancellation procedure, as shown in [6].

Having orthogonalized the basis functions, they can then be used for learning the SI channel coefficients with the LMS algorithm. Now, the input vector of the LMS filter, containing all the orthogonalized basis functions, is defined as follows:

$$\tilde{\Psi}(n) = [\tilde{\psi}(n+M_1) \ \tilde{\psi}(n+M_1-1) \ \cdots \ \tilde{\psi}(n-M_2)].$$

Then, denoting the LMS channel estimate in the receiver after  $n$  iterations by  $\hat{\mathbf{h}}(n)$  (where  $n = 0, 1, \dots, N-1$ ), the signal after cancellation is given by

$$y_{\text{DC}}(n) = y_{\text{ADC}}(n) - \tilde{\Psi}(n)\hat{\mathbf{h}}(n). \quad (5)$$

Subsequently, the LMS algorithm updates the SI channel estimate using the following rule [3], [12]:

$$\hat{\mathbf{h}}(n+1) = \hat{\mathbf{h}}(n) + \mathbf{M}y_{\text{DC}}(n)\tilde{\Psi}^H(n), \quad (6)$$

where  $\mathbf{M}$  is a diagonal matrix containing the step sizes for the different orthogonalized basis functions. In general, the channel estimate can be initialized simply as  $\hat{\mathbf{h}}(0) = \mathbf{0}$ .

As shown in [3], the benefit of the LMS algorithm is that it is computationally more efficient than performing the estimation with, for example, the least squares (LS). Moreover, the LMS-based digital canceller is also capable of tracking the SI channel under time-varying conditions, unlike an LS estimator

which assumes the SI channel to be static during the whole observation period of  $N$  samples. However, as is well known in estimation theory, with a sufficient amount of learning data and Gaussian-distributed noise, the variance of the channel estimate given by the LMS algorithm is higher than that given by the LS estimator [14, p. 397]. This is an inherent cost for the many upsides of the LMS canceller.

#### IV. MEASUREMENTS ON PROTOTYPE IMPLEMENTATIONS

The overall cancellation performance of the digital SI cancellers is evaluated with two different prototype implementations, reported in [5] and [6]. Here, only the cancellation performance of the linear and nonlinear digital cancellers is demonstrated as the PA-induced nonlinear distortion is the dominant impairment in these prototypes, owing to the low-cost PA. In contrast, I/Q imbalance is not an issue due to the high image rejection ratio of the National Instruments vector signal transceiver (PXIe-5645R) used in the measurements.

The prototype implementation in [5] represents a single-antenna IBFD transceiver, which complements the physical isolation provided by a circulator with two active cancellers: the RF canceller and the digital canceller. As opposed to this, the prototype in [6] is constructed around a high-isolation relay antenna, which means that no RF cancellation is required as the antenna itself provides the necessary SI suppression in the analog domain. Therefore, this prototype only has an active digital canceller. The more detailed measurement parameters of both of these prototypes can be found in [3].

Investigating first the single-antenna prototype of [5], Figs. 1(a)–(c) show the power spectral densities (PSDs) of the SI signal at different interfaces of the IBFD transceiver for the three considered bandwidths, the signal powers being referred to the RX input. Investigating first the 20-MHz case in Fig. 1(a), the residual SI power after RF cancellation is  $-61$  dBm, which is clearly above the receiver noise floor and hence calls for further cancellation in the digital domain. It can firstly be observed that, due to the highly nonlinear low-cost PA, the linear digital canceller is not capable of fully suppressing the residual SI, achieving roughly 18 dB of cancellation. On the other hand, the nonlinear canceller manages to suppress the SI to the level of the receiver noise floor, canceling it by over 25 dB. Hence, the total amount of obtained SI cancellation is 94 dB, of which 20 dB is physical isolation from the antenna and the circulator, while 47 dB of the overall suppression is provided by the RF canceller.

The nonlinear digital canceller copes well also with the wider bandwidths, since the residual SI is still cancelled close to the receiver noise floor in the 40-MHz and 80-MHz cases, as can be observed from Figs. 1(b) and 1(c). Moreover, similar to the 20-MHz scenario, the residual SI after linear digital cancellation is roughly 10 dB above the noise floor also with these wider bandwidths, indicating that nonlinear modeling is indeed necessary. With a bandwidth of 40 MHz, the total amount of SI cancellation is therefore 92 dB, of which 44 dB is provided by the RF canceller, while the nonlinear digital canceller suppresses the SI by 26 dB. Correspondingly, in

the 80-MHz scenario, the SI is suppressed by 88 dB in total, consisting of 41 dB of RF cancellation and 25 dB of nonlinear digital cancellation. Thus, high SI cancellation performance is achieved even under wideband operation.

Considering then the IBFD relay prototype in [6], the PSDs of the signal after the different SI cancellation stages are shown in Figs. 1(d)–(f), using again the RX input as the reference point for the different power levels. Investigating first the isolation provided by the antenna, it can be observed that it is in the order of 60 dB for each bandwidth when considering also the cable losses in the RX path (4 dB). Hence, the power of the residual SI signal entering the digital domain is roughly  $-40$  dBm in all the cases, which is already sufficiently low for the RX chain to operate without saturation or excessive distortion. Consequently, no active cancellation is required before the analog-to-digital conversion.

Analyzing then the digital cancellation performance of the relay prototype in [6], it is clear that also now the linear digital canceller is incapable of fully suppressing the residual SI. Namely, the residual SI power after linear cancellation is still 10–15 dB above the receiver noise floor, rendering the IBFD operation infeasible. On the other hand, the nonlinear canceller with LMS-based parameter learning is capable of very efficient SI cancellation with all the considered bandwidths, reducing the overall noise-plus-interference power practically to the level of the receiver noise floor. Hence, the amount of digital SI cancellation is beyond 40 dB for each considered bandwidth and, taking into account the RX cable losses, the overall amounts of SI suppression are 106 dB, 103 dB, and 100 dB over 20 MHz, 40 MHz, and 80 MHz, respectively.

In general, these measurement results obtained with two different IBFD prototypes demonstrate the flexibility of the developed LMS-based nonlinear digital cancellation algorithm, as it is shown to be capable of efficient SI cancellation both with and without a RF cancellation stage. Indeed, with the considered transmit powers of 6–24 dBm and instantaneous bandwidths of 20–80 MHz, the implemented IBFD prototypes are capable of canceling the residual SI to the level of the receiver noise floor when using the developed nonlinear digital canceller with LMS-based parameter learning. For more detailed discussion, refer to [3], [5], [6].

#### V. SELF-BACKHAULING FULL-DUPLEX ACCESS NODE WITH MASSIVE ANTENNA ARRAYS

Wireless inband self-backhauling has recently been considered as a possible option for decreasing the cost of the densely deployed cellular networks of the future [3], [10]. It would allow the access nodes (ANs) to backhaul all the data with a backhaul node (BN) without requiring any wired data link, significantly reducing deployment costs. What is more, utilizing the IBFD technology in this context would allow the AN to simultaneously serve the UL and DL UEs on the same frequency band, further improving the spectral efficiency of such a network. Therefore, IBFD self-backhauling facilitates higher data rates while also reducing the associated costs, making it an intriguing concept for the future 5G systems.

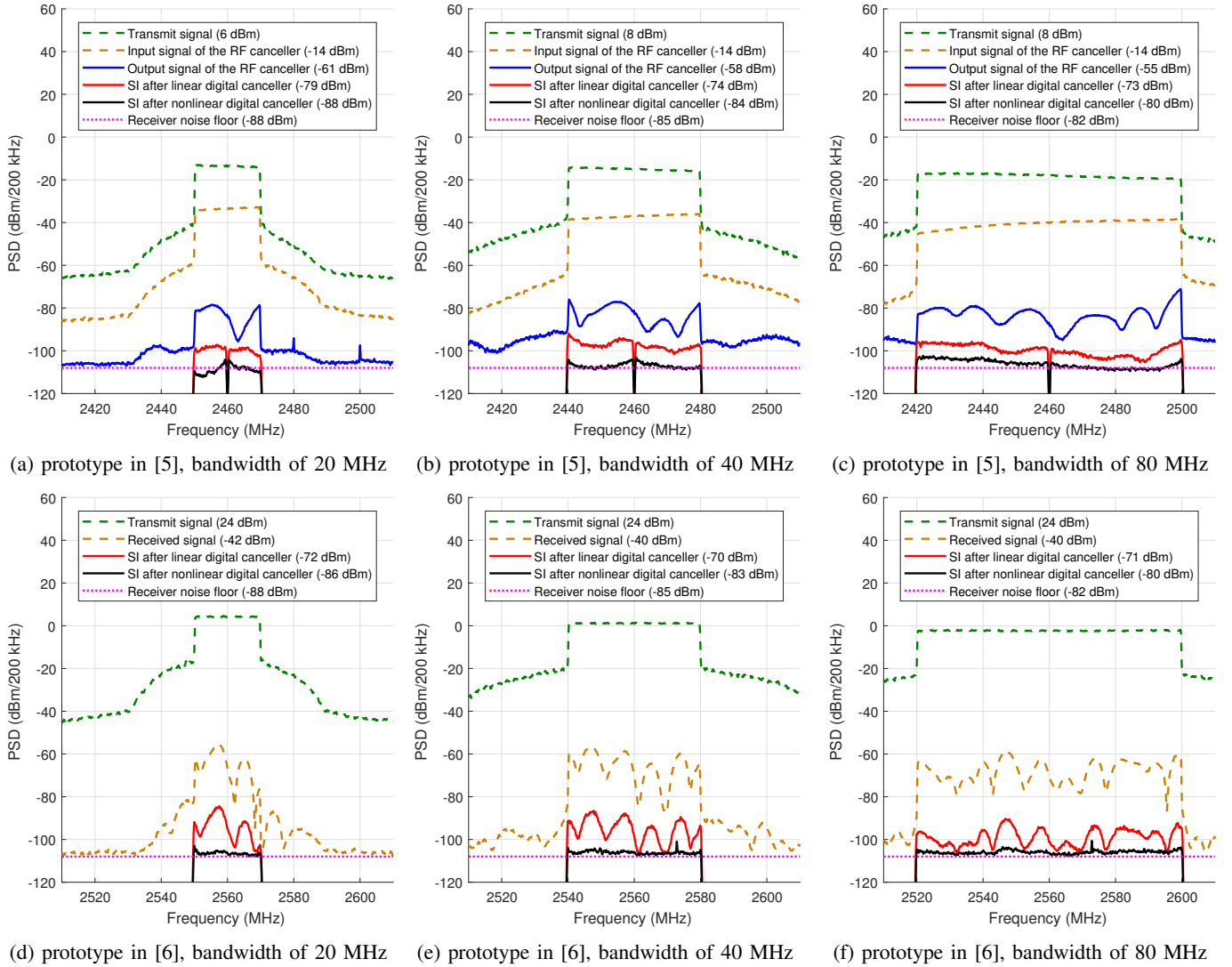


Fig. 1: The power spectral densities of SI signals after the different cancellation stages for the prototypes in [5] and [6].

In particular, let us consider the system depicted in Fig. 2, where an IBFD-capable AN with massive TX and RX antenna arrays is serving half-duplex-capable single-antenna UL and DL UEs while also using the same frequency band and antenna arrays for backhauling the data. The wireless backhaul link is maintained by exchanging data with an IBFD-capable MIMO BN, which then further forwards the data either via a wired or wireless connection to the core network. The considered system is analyzed in terms of minimizing the transmit powers under some given Quality-of-Service (QoS) requirements, defined as minimum UL and DL data rates. Moreover, the IBFD solution is compared to two references: *the half-duplex scheme* and *the hybrid relay scheme*. The former relies solely on traditional half-duplex communication while in the latter the AN acts as a one-directional full-duplex relay.

The proposed system is evaluated with the help of Monte Carlo simulations, considering the three different communications schemes. In the simulations, the UEs are randomly positioned into a circular cell of given size, at the center

of which is the AN. The path losses for the different links are then calculated based on the corresponding distances and the adopted path loss model. By calculating the feasibility boundaries and optimal transmit powers over various random network realizations, the cumulative distribution functions (CDFs) of the corresponding quantities can then be obtained.

Analyzing the transmit power efficiency of the different schemes, the CDFs of the optimal transmit powers for the different communicating parties are shown in Fig. 3, using the default system parameters defined in [3]. Firstly, it can be observed that the full-duplex scheme is capable of operating with the lowest transmit powers. However, the drawback of the full-duplex scheme is its inability to achieve the QoS requirements under all network geometries, evidenced by the fact that the CDFs converge to a value less than one. With these particular network geometries, performing IBFD self-backhauling is fundamentally infeasible.

The hybrid relay scheme is the next best option when considering the overall transmit power usage, although it is

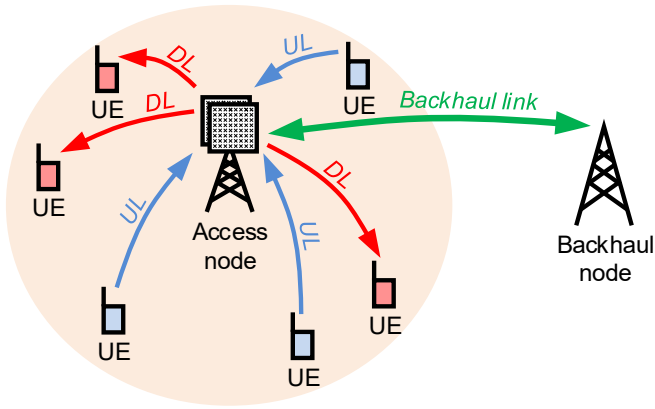


Fig. 2: Wireless self-backhauling with an IBFD-capable access node.

outperformed by the half-duplex scheme in terms of the UE transmit power consumption. The latter is simply a result of the formulation of the optimization problem, which aims at minimizing the *total* transmit power consumption. With these example system parameters, this incidentally results in lower UE transmit powers in the half-duplex scheme even though the hybrid relay scheme consumes less transmit power in total. Another drawback of the hybrid relay scheme is its inability to fulfill the QoS requirements under some network geometries, similar to the full-duplex scheme.

In general, it can be concluded that the full-duplex scheme provides the highest transmit power efficiency when operating under some given QoS requirements. However, care must be taken to ensure that the system parameters are such that the full-duplex scheme does not suffer from the problem of infeasibility. If, however, this cannot be ensured, then the hybrid relay scheme is perhaps the more preferable option as it is somewhat more robust in obtaining the given data rate requirements under different circumstances.

## VI. CONCLUSION

In this paper, we presented an overview of the findings and results reported in [3]. Firstly, we discussed the significant analog impairments that affect the SI waveform upon digital cancellation, proposing also signal models that incorporate the impairments in question. Of these, the nonlinear signal model was evaluated with real-life RF measurements that incorporated also other analog SI cancellation stages. Using the nonlinear digital canceller, the SI was suppressed by as much as 106 dB in total, canceling it nearly perfectly. In addition, we also investigated how to utilize the full-duplex technology on a system-level for performing wireless self-backhauling with simultaneous uplink and downlink connectivity. The results indicate that the full-duplex capability facilitates the use of lower transmit powers without sacrificing the QoS.

## ACKNOWLEDGMENT

This work was supported by the Academy of Finland (under the projects #301820, #304147, and #310991), the Finnish Funding Agency for Technology and Innovation (Tekes, under the TAKE-5 project), and Tampere University of Technology Graduate School.

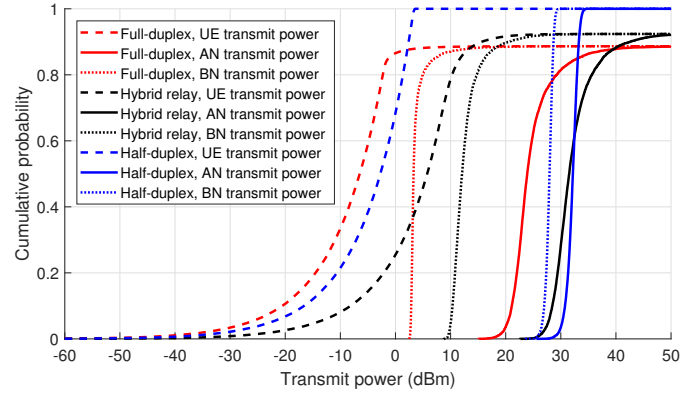


Fig. 3: CDFs of the transmit powers of the individual communicating parties with typical system parameters.

## REFERENCES

- [1] A. Sabharwal, P. Schniter, D. Guo, D. W. Bliss, S. Rangarajan, and R. Wichman, "In-band full-duplex wireless: Challenges and opportunities," *IEEE Journal on Selected Areas in Communications*, vol. 32, no. 9, pp. 1637–1652, Sep. 2014.
- [2] D. Bharadia, E. McMillin, and S. Katti, "Full duplex radios," in *Proc. SIGCOMM'13*, Aug. 2013, pp. 375–386.
- [3] D. Korpi, "Full-duplex wireless: Self-interference modeling, digital cancellation, and system studies," Ph.D. dissertation, Tampere University of Technology, Dec. 2017.
- [4] D. Korpi, L. Anttila, V. Syrjälä, and M. Valkama, "Widely linear digital self-interference cancellation in direct-conversion full-duplex transceiver," *IEEE Journal on Selected Areas in Communications*, vol. 32, no. 9, pp. 1674–1687, Sep. 2014.
- [5] D. Korpi, J. Tamminen, M. Turunen, T. Huusari, Y.-S. Choi, L. Anttila, S. Talwar, and M. Valkama, "Full-duplex mobile device: Pushing the limits," *IEEE Communications Magazine*, vol. 54, no. 9, pp. 80–87, Sep. 2016.
- [6] D. Korpi, M. Heino, C. Icheln, K. Haneda, and M. Valkama, "Compact inband full-duplex relays with beyond 100 dB self-interference suppression: Enabling techniques and field measurements," *IEEE Transactions on Antennas and Propagation*, vol. 65, pp. 960–965, Feb. 2017.
- [7] M. Heino, D. Korpi, T. Huusari, E. Antonio-Rodríguez, S. Venkatasubramanian, T. Riihonen, L. Anttila, C. Icheln, K. Haneda, R. Wichman, and M. Valkama, "Recent advances in antenna design and interference cancellation algorithms for in-band full-duplex relays," *IEEE Communications Magazine*, vol. 53, no. 5, pp. 91–101, May 2015.
- [8] D. Korpi, T. Riihonen, V. Syrjälä, L. Anttila, M. Valkama, and R. Wichman, "Full-duplex transceiver system calculations: Analysis of ADC and linearity challenges," *IEEE Transactions on Wireless Communications*, vol. 13, no. 7, pp. 3821–3836, Jul. 2014.
- [9] D. Korpi, L. Anttila, and M. Valkama, "Nonlinear self-interference cancellation in MIMO full-duplex transceivers under crosstalk," *EURASIP Journal on Wireless Communications and Networking*, vol. 2017, no. 1, p. 24, Feb. 2017.
- [10] D. Korpi, T. Riihonen, A. Sabharwal, and M. Valkama, "Transmit power optimization and feasibility analysis of self-backhauling full-duplex radio access systems," *IEEE Transactions on Wireless Communications*, in press, 2018.
- [11] L. Anttila, D. Korpi, V. Syrjälä, and M. Valkama, "Cancellation of power amplifier induced nonlinear self-interference in full-duplex transceivers," in *Proc. 47th Asilomar Conference on Signals, Systems and Computers (ASILOMAR)*, Nov. 2013, pp. 1193–1198.
- [12] D. Korpi, Y.-S. Choi, T. Huusari, S. Anttila, L. Talwar, and M. Valkama, "Adaptive nonlinear digital self-interference cancellation for mobile inband full-duplex radio: Algorithms and RF measurements," in *Proc. IEEE Global Communications Conference (GLOBECOM)*, Dec. 2015.
- [13] M. Emara, M. Faerber, L. G. Baltar, J. Nossek, and K. Roth, "Non-linear digital self-interference cancellation with reduced complexity for full duplex systems," in *Proc. International ITG Workshop on Smart Antennas (WSA)*, Mar. 2017.
- [14] S. Haykin, *Adaptive Filter Theory*, 3rd ed. Prentice Hall, 1996.